Theoretical and Applied Mechanics Letters 11 (2021) 100305

Contents lists available at ScienceDirect

Theoretical and Applied Mechanics Letters

journal homepage: www.elsevier.com/locate/taml

Letter

Validation of actuator disc circulation distribution for unsteady virtual blades model

A. N. Kusyumov [a,*], S. A. Kusyumov [a], S. A. Mikhailov [a], G. N. Barakos [b]

[a] Kazan National Research Technical University n.a. A N Tupolev, Russia
[b] Glasgow University, Glasgow, UK

ARTICLE INFO

Article history:
Received 8 August 2021
Revised 21 September 2021
Accepted 12 October 2021
Available online 23 November 2021

Keywords:
Surface circulation distribution
Unsteady actuator disk model
Blade tip vortices reproduction

ABSTRACT

The actuator disc method is an engineering approach to reduce computer resources in computational fluid dynamics (CFD) simulations of helicopter rotors or aeroplane propellers. Implementation of an actuator disc based on rotor circulation distribution allows for approximations to be made while reproducing the blade tip vortices. Radial circulation distributions can be formulated according to the nonuniform Heyson-Katzoff "typical load" in hover. In forward flight, the nonuniform disk models include "azimuthal" sin and cos terms to reproduce the blade cyclic motion. The azimuthal circulation distribution for a forward flight mode corresponds to trimmed conditions for the disk rolling and pitching moments. The amplitude of the cos harmonic is analysed and compared here with presented in references data and CFD simulations results.

One of the primary requirements in helicopter design is the estimation of the rotor effect on the helicopter fuselage. In particular, the fuselage surface pressure distribution can be used as initial data for structural analyses. The actuator disc (AD) method is a mathematical approach in computational fluid dynamics (CFD) to approximate a helicopter rotor or an airplane propeller. For this purpose, the Navier-Stokes or Reynolds averaged Navier-Stokes (RANS) equations are modified with a source terms distribution in the momentum equations. The "intensity" of the source terms is determined in the form of a "pressure jump" across the AD surface in accordance to the rotor thrust force. Since no surface is needed in the grid, the position of the sources reproducing the blades location can be changed without transformation of the initial grid.

In some CFD solvers (commercial ANSYS fluent CFD code, for example) the AD conception is realized in the form of a special type of boundary condition applied on the infinitely thin AD surface, localized at (and instead of) the fully resolved rotor disk.

Classical helicopter AD models provide a steady-state formulation of the RANS equations to estimate a time-averaged action of the rotor downwash on the helicopter fuselage and its surface elements. Within the classical AD models, the source terms are continuously distributed on the AD surface.

A more realistic approach for simulation of the unsteady space structure of the helicopter rotor wake is based on a variable and space localized source distribution similar to the fully resolved rotor blades planform. Such methods require solution of the unsteady Reynolds averaged Navier-Stokes (URANS) equations and are called as the actuator-blade methods.

For example, with the actuator-lines method [1,2] the rotor blades action is simulated by forces acting along filaments sources lines. Body forces are typically derived from the blade element momentum (BEM) method. This classic BEM method is based requires corrections particularly near the blade tip region [3]. In Lynch et al. [4] it is noted that such correction can be applied using Prandtl's approach [5].

An alternative approach which reproduces the flow structure is the unsteady AD method: the disk surface is divided in the azimuthal direction with a time-varied pressure jump across the AD surface elements [4, 6]. In references [7–9], such approach was termed unsteady virtual blades actuator (VBA) model. In Ref. [8] the AD surface was divided in 4 sectors according to the rotor blades number (Fig. 1).

In forward flight the nonuniform AD models include "azimuthal" terms reproducing the blade cyclic. The amplitudes of the azimuthal terms depend on the AD models and should be adjusted to provide trimmed flight disk loading. Reference [9] presents the AD mathematical formulations and comparison of several AD models, based on prescribed AD circulation distributions. The AD1

* Corresponding author.
E-mail address: postbox7@mail.ru (A. N. Kusyumov).

https://doi.org/10.1016/j.taml.2021.100305

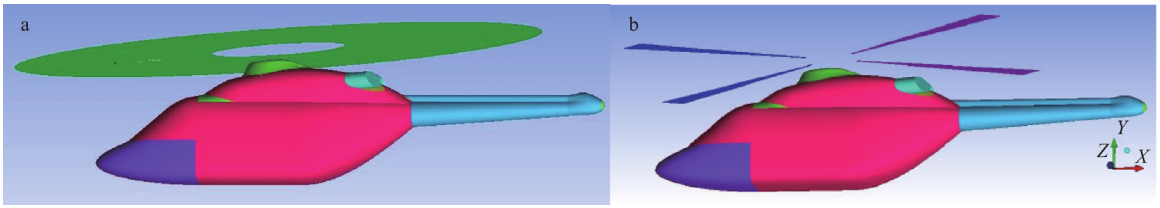

Fig. 1. a CAD model image of fuselage with the classical AD; b Unsteady AD.

model presented in Ref. [9] takes into consideration only the azimuthal variation of the rotor circulation distribution. For the AD2 model the AD loading is determined with the Blade Element Theory. A more complicated model AD3 is based on the "typical" circulation distribution [10]. The formulation of that model takes into account both azimuthal and radial circulation distributions and is described in detail in Ref. [11].

Another (different from Ref. [11]) approach, termed AD4, that also accounts for the radial and azimuthal circulation distribution, is presented in Ref, [9]. The AD loadings for different models are compared in Ref. [9] by the rotor surface normal force distribution obtained with numerical simulation for the PSP rotor [12].

It should be noted that two kinds of "trimming coefficients", determining the amplitude of the blade cyclic motion are offered [9]. A difference between the trimming coefficients is determined by a functional dependence (linear or nonlinear) on the rotor advance ratio. The goal of this paper is the comparative analysis of the AD loading for the AD4 model with the linear and nonlinear forms of the trimming coefficients. For prescribed flight conditions the circulation distribution of the AD4 model is compared to the circulation distribution obtained with vortex theory [13]. In addition the AD surface pressure distribution is compared to PSP rotor CFD simulation results (unlike Ref. [9], which considered a comparison with the surface normal force coefficient).

A widely accepted AD model, expresses the AD loading of a forward flying rotor as a function of the disk radius r and azimuth angle Ψ:

$$\Delta p(r,\Psi) = \Delta p_0 + \Delta p_{1s}\sin(r,\Psi) + \Delta p_{2s}\cos(r,\Psi), \tag{1}$$

where the functions $\sin(r,\Psi)$ and $\cos(r,\Psi)$ determine the sin and cos pressure oscillations, and the coefficients Δp_0, Δp_{1s}, and Δp_{2s} depend on the rotor geometry and flight conditions. Using the rotor circulation function $\Gamma(r,\Psi)$ the local loading can be written as

$$\Delta p(r,\Psi) = \frac{1}{2\pi r}\rho U(r,\Psi)\Gamma(r,\Psi), \tag{2}$$

where

$$U(r,\Psi) = r + \Omega R\mu\sin\Psi, \tag{3}$$

here ρ is the air density, Ω is the blade rotational speed, R is the rotor disk radius, and μ is the rotor advance ratio:

$$\mu = \frac{V\cos(\alpha_r)}{V_{\text{tip}}},$$

where $V_{\text{tip}} = \Omega R$ is the blade tip speed, V is the forward rotor velocity, and α_r is the rotor disk plane tilt angle (positive for forward tilt).

The simplified circulation distribution (AD1 model) can be written as [9,13]:

$$\Gamma(\Psi) = \Gamma_1\bar{\gamma}_1(\Psi), \tag{4}$$

while

$$\Gamma_1 = \frac{3\pi C_T\Omega R^2\sqrt{4-9\mu^2}}{2\left[2\sqrt{4-9\mu^2}-1\right]}, \bar{\gamma}_1(\Psi) = \frac{1}{1+\frac{3}{2}\mu\sin\Psi}, \tag{5}$$

where C_T is the rotor trust coefficient determined by the rotor thrust T:

$$C_T = \frac{2T}{\pi\rho\Omega^2R^4}.$$

A more advanced model is based on a "typical" circulation distribution [10]. According to Ref. [9] the circulation distribution also depends on the normalized radial coordinate $\bar{r} = r/R$, and can be approximated as:

$$\Gamma(\bar{r},\Psi) = \Gamma_4\bar{\gamma}_4(\bar{r},\Psi), \tag{6}$$

here

$$\Gamma_4 = \frac{\pi V^2}{\Omega}\frac{C_T}{\mu^2}, \tag{7}$$

$$\bar{\gamma}_4(\bar{r},\Psi) = \bar{\gamma}_r(\bar{r}) + \bar{\gamma}_s(\bar{r},\mu)\sin\Psi + \bar{\gamma}_c(\bar{r},\mu)\cos(2\Psi). \tag{8}$$

The azimuthal variation of the dimensionless disk circulation distribution $\bar{\gamma}_4(\bar{r},\Psi)$ is determined by the rotor advance ratio μ and does not depend on the rotor thrust coefficient that is accounted by the Γ_4 term. The dimensionless disk circulation distribution $\bar{\gamma}_r(\bar{r})$ for the hover mode is determined as [10]:

$$\bar{\gamma}_r(\bar{r}) = \frac{12}{5}\bar{r}^2\left(2-\bar{r}^2-\bar{r}^4\right), \tag{9}$$

whereas the sin $\bar{\gamma}_s(\bar{r},\mu)$, and the cos $\bar{\gamma}_c(\bar{r},\mu)$ components allow for simulation of the trimmed rotor in forward flight and can be written in the form [9]:

$$\bar{\gamma}_s(\bar{r},\mu) = K(\mu)\bar{\gamma}_r(\bar{r})\bar{r}^{-1}\left(1-\frac{14}{5}\bar{r}^2\right), \tag{10}$$

$$\bar{\gamma}_c(\bar{r},\mu) = K(\mu)\bar{\gamma}_r(\bar{r})\left(1-W(\mu)\bar{r}^2\right). \tag{11}$$

Two kinds of trimming coefficients $K(\mu)$ and $W(\mu)$ can be determined for the sin and cos harmonic components [9] as linear and nonlinear functions of the advance ratio:

$$K(\mu) = K_{41}(\mu) = \frac{125}{57}\mu, \quad W = W_{41} = \frac{25}{13}, \tag{12}$$

$$K(\mu) = K_{42}(\mu) = \frac{250\mu}{3(15\mu+38)}, \quad W = W_{42} = \frac{16}{13}. \tag{13}$$

Substitution of Eqs. (12) and (13) into Eqs. (10) and (11) allows determination two kinds of functions for the dimensionless AD surface circulation distribution: $\bar{\gamma}_{41}(\bar{r},\Psi)$ and $\bar{\gamma}_{42}(\bar{r},\Psi)$.

One should note that both kinds trimming coefficients determine the AD loading distribution are comparable, in general, to the CFD results. The radius-averaged azimuthal circulation distribution can be considered for clarification of the trimming coefficients choice. One can determine the averaged 1D function

$$\bar{\gamma}_{4a}(\Psi) = 2\int_0^1 \bar{\gamma}_4(\bar{r},\Psi)\bar{r}\mathrm{d}\bar{r}, \tag{14}$$

to compare with the simplest $\bar{\gamma}_1(\Psi)$ dimensionless AD circulation. Substituting Eqs. (10) and (11) into Eqs. (14) and (15) gives a general expression

$$\bar{\gamma}_{4a}(\Psi) = 1 - \frac{1072}{2625}K(\mu)\sin\Psi - \frac{1}{25}K(\mu)(13W-25)\cos(2\Psi).$$

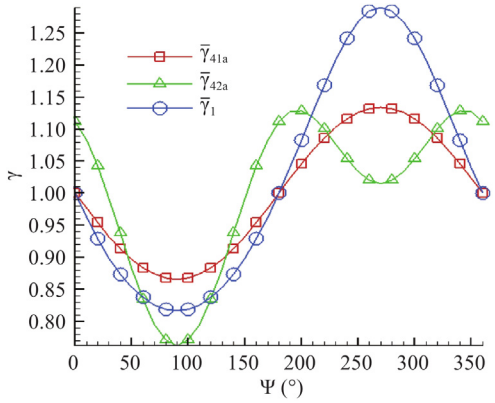

Fig. 2. Comparison of the dimensionless AD circulation azimuthal distributions corresponded to the $\bar{\gamma}_1, \bar{\gamma}_{41a}, \bar{\gamma}_{42a}$functions.

(15)

Substituting Eqs. (12) and (13) into Eq. (15) gives respectively

$$\bar{\gamma}_{41a}(\Psi) = 1 - \frac{1072\mu}{1197}\sin\Psi,$$

and

$$\bar{\gamma}_{42a}(\Psi) = 1 - \frac{2144\mu}{63(15\mu+38)}\sin\Psi + \frac{30\mu}{(15\mu+38)}\cos(2\Psi).$$

Figure 2 shows the function $\bar{\gamma}_1(\Psi)$ in comparison to the averaged 1D functions $\bar{\gamma}_{41a}(\Psi)$, and $\bar{\gamma}_{42a}(\Psi)$ distribution for the rotor advance ratio μ of 0.15.

From Fig. 2, it follows that the and $\bar{\gamma}_1(\Psi)$ and $\overline{\varphi}_{41a}(\Psi)$ function have two extremums, unlike the $\bar{\gamma}_{42a}(\Psi)$ function, which has four extremums and one can expect that the $\bar{\gamma}_{42a}(\Psi)$ function allows for better reproduction of real main rotor disk properties.

In Fig. 3, the dimensionless circulation distributions $\bar{\gamma}_{41}(\bar{r},\Psi)$ and $\bar{\gamma}_{42}(\bar{r},\Psi)$ are shown for $\mu = 0.1$. Figure 3 shows a discrepancy between the dimensionless $\bar{\gamma}_{41}(\bar{r},\Psi)$ and $\bar{\gamma}_{42}(\bar{r},\Psi)$ circulation distributions at the retreating blade area. Due to the different sine cosine harmonic circulation components the AD model with the $\bar{\gamma}_{41}$ circulation distribution is slightly higher in comparison with the $\bar{\gamma}_{42}$ circulation near $\approx 270°$.

To validate the obtained disk load distributions one can analyze the rotor AD surface load distribution determined by the $\bar{\gamma}_{41}(\bar{r},\Psi)$ and $\bar{\gamma}_{42}(\bar{r},\Psi)$ functions in comparison with data presented in references. The theoretical circulation distribution obtained from the

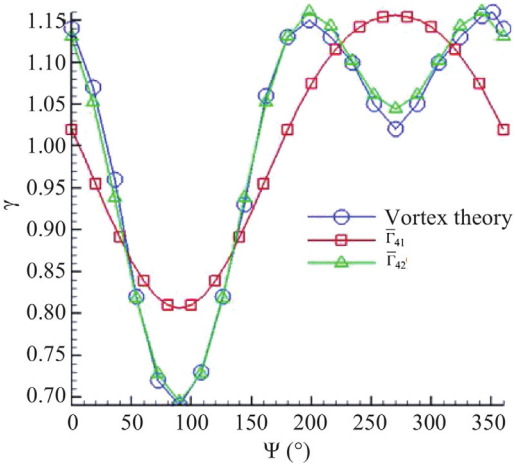

Fig. 4. Comparison of the normalized AD circulation azimuthal distributions at the $\bar{r} = 0.7$ section: data for $\bar{\Gamma}_{41}$, $\bar{\Gamma}_{42}$ and from (**Vortex theory**).

vortex theory is presented in Ref. [13] at the main rotor disk section $\bar{r} = 0.7$ for the rotor parameters: the rotor solidity $\sigma = 0.07$, the rotor trust C_T coefficient of 0.012 and the advancing ratio of 0.15.

Figure 4 presents the normalized $\bar{\gamma}_{41}(\bar{r},\Psi)$ and $\bar{\gamma}_{42}(\bar{r},\Psi)$ functions compared with a theoretical circulation distribution. The relative theoretical circulation distribution is presented in Ref. [13] in the form

$$\overline{\Gamma}(\bar{r}=0.7,\Psi) = 1 + \overline{\Gamma}_1\sin\Psi + \overline{\Gamma}_2\cos(2\Psi),$$

where $\bar{\Gamma}_1$, and $\bar{\Gamma}_2$ are constant. For comparison to the theoretical circulation distribution the functions $\bar{\gamma}_{41}(\bar{r}=0.7,\Psi)$ and $\bar{\gamma}_{42}(\bar{r}=0.7,\Psi)$ are written in the normalized form

$$\bar{\Gamma}_{41}(\bar{r}=0.7,\Psi) = \frac{\bar{\gamma}_{41}(\bar{r}=0.7,\Psi)}{\bar{\gamma}_r(\bar{r}=0.7)},$$

$$\bar{\Gamma}_{42}(\bar{r}=0.7,\Psi) = \frac{\bar{\gamma}_{42}(\bar{r}=0.7,\Psi)}{\bar{\gamma}_r(\bar{r}=0.7)},$$

where the function $\bar{\gamma}_r(\bar{r}=0.7)$ is determined by Eq. (9) for $\bar{r} = 0.7$.

Figure 4 shows, that the normalized $\bar{\Gamma}_{42}(\bar{r}=0.7,\Psi)$ distribution agrees very well with the vortex theory results. The trimming coefficients determined by expressions Eq. (13) (nonlinear form) thus provide better agreement of the rotor disk circulation distribution in comparison with the coefficients of Eq. (12) (linear dependence on the advance ratio).

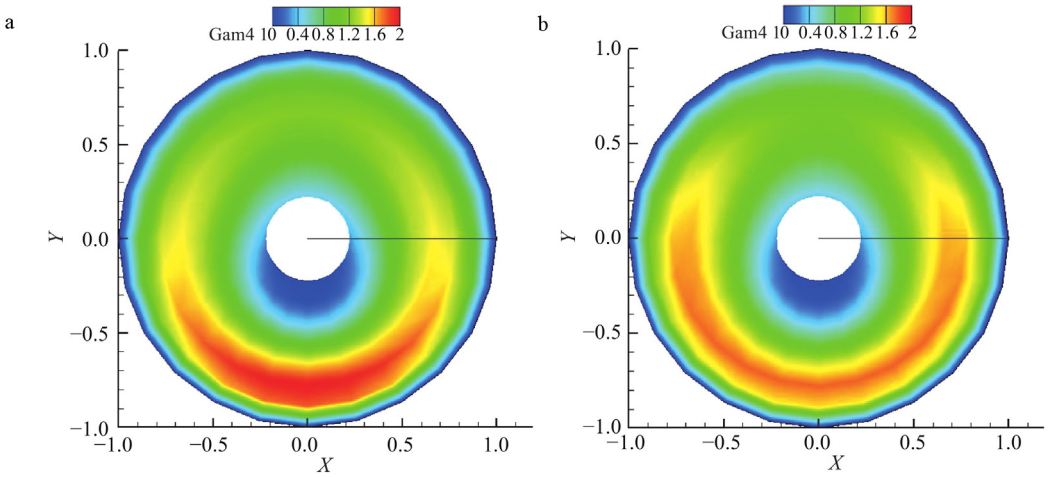

Fig. 3. **a** The dimensionless AD circulation distribution determined by $\bar{\gamma}_{41}(\bar{r},\Psi)$; **b** $\bar{\gamma}_{42}(\bar{r},\Psi)$ function.

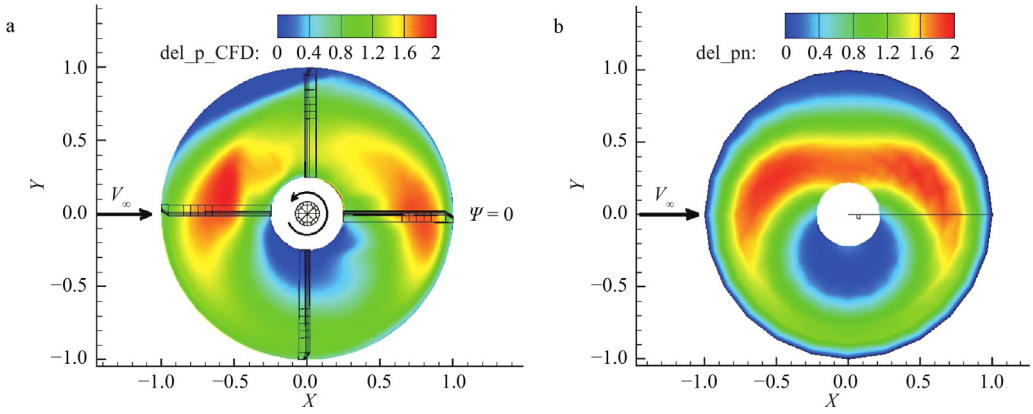

Fig. 5. **a** The normalized pressure jump distribution based on CFD data from [9]; **b** The AD model with the $\bar{\gamma}_{42}$ circulation distribution.

The theoretical AD loading can be compared with CFD results. For CFD simulation the four-bladed PSP [12] rotor was considered (details of the rotor geometry, simulation conditions and brief description of a CFD solver are presented). In Ref. [9] the theoretical and CFD normal force coefficient distributions for the PSP rotor were also compared. In Fig. 5a comparison of the AD loadings are considered for the surface pressure jump across the disk (whichisused as boundary condition in VBA models).The dimensionless pressure jump distribution on the rotor disk surface is shown for$C_T = 0.016$, $\mu = 0.35$. In Fig. 5a the dimensionless pressure jump $\Delta\bar{p}_{\mathrm{CFD}}(\bar{r}, \Psi)$ is determined by the normalized rotor disk load $C_n M^2_{\mathrm{tip}}$:

$$\Delta\overline{p}_{\mathrm{CFD}}(\bar{r}, \Psi) = \frac{2\Delta p_{CFD}(\bar{r}, \Psi)}{\rho V^2_{\mathrm{tip}}} = C_n M^2_{\mathrm{tip}} \frac{\sigma}{2\bar{r} C_T M^2_{\mathrm{tip}}},$$

here M_{tip} is the blade tip Mach number, and C_n is the normal force coefficient. Figure 5b shows the obtained distribution

$$\Delta\overline{p}(\bar{r}, \Psi) = \frac{2p(r, \Psi)}{\rho V^2_{\mathrm{tip}}},$$

where $\Delta p(r, \Psi)$ is determined by the expression (2) for the $\bar{\gamma}_{42}(\bar{r}, \Psi)$ circulation distribution.

Comparison of the CFD simulation results to the obtained for $\bar{\gamma}_{42}(\bar{r}, \Psi)$ pressure jump distribution shows a satisfactory agreement. The VBA model approach is based on "typical" [10] circulation distributions on the rotor disk and does not take into account the specific blade design or any particular rotor trimming method. For this reason, the considered AD model shows some discrepancy of the rotor disk load near the azimuth angle Ψ of 90° compared to the CFD data. Nevertheless, the AD model predicted the high disk load for $\Psi \approx 45°$ and 135° at the disk radius $0.75R$ and the lower values of the disk load near the rotor root part for $\Psi \approx 45°$.

Circulation distribution on the surface nonuniformly loaded actuator disk model is analyzed developed using the “typical law” of the helicopter main rotor disk circulation distribution. The actuator disk model contains “trimming coefficients”, which determine disk circulation distribution taking into account the sin and cos circulation components. Circulation distribution on the disk surface is analyzed for two kinds of the trimming coefficients, which linear or nonlinear depend on the rotor advance ratio.

Both linear and nonlinear models yield the assigned thrust coefficient value and satisfied the trimming conditions of the AD load for forward flight. However, the nonlinear AD model better agrees with the vortex theory prediction and with the rotor CFD simulation results. Comparison to the vortex theory results at the 75% of the rotor radius shows good agreement for the azimuthal circulation distribution, including peak to peak values and their location. Comparison to the CFD simulation results for the four-bladed rotor shows that the AD model predicted well the disk load for different azimuth angles and rotor disk radius, excluding the azimuth area near 90°.

Declaration of Interest Statement

We confirm that the manuscript has been read and approved by all named authors and that there are no other persons who satisfied the criteria for authorship but are not listed. We further confirm that the order of authors listed in the manuscript has been approved by all of us.

Declaration of Competing Interest

The authors declare no conflict of interest.

Acknowledgement

Work of Russian coauthors was supported by the grant "FZSU-2020-0021" (No. 075-03-2020-051/3 from 09.06.2020) of the Ministry of Education and Science of the Russian Federation.

References

[1] J.N. Sorensen, W.Z. Shen, Numerical modeling of wind turbine wakes, J. Fluids Eng. 124 (2002) 393–399.
[2] M.J. Churchfield, S.J. Schreck, L.A. Martinez, et al., An advanced actuator linemethod for wind energy applications and beyond, in: 35th Wind Energy Symposium, Grapevine, Texas, USA, 2017, pp. 1–20.
[3] W.Z. Shen, J.H. Zhang, J.N. Sorensen, The actuator surface model: a new Navier–Stokes based model for rotor computations, J. Sol. Energy Eng. 131 (1) (2009) 9.
[4] C.E. Lynch, D.T. Prosser, M.J. Smith, An efficient actuating blade model for unsteady rotating system wake simulations, Comput. Fluids 92 (2014) 138–150.
[5] J.G. Leishman, in: Principles of helicopter aerodynamics, 2nd ed., Cambridge University Press, Cambridge, 2006, pp. 74–77.
[6] D. O'Brien, Analysis of computational modeling techniques for complete rotorcraft configurations [Dissertation], Georgia Institute of Technology, 2006.
[7] P. Li, Q. Zhao, Q. Zhu, CFD calculations on the unsteady aerodynamic characteristics of a tilt-rotor in a conversion mode, CJA 28 (6) (2015) 1593–1605.
[8] S.Mikhailov A.Kusyumov, K. Phayzullin, G. Barakos, S. Kusyumov, E. Romanova, E. Lopatin, Main rotor-body action for virtual blades model, EPJ Web Conf. 143 (2017) 1–6.

[9] G.N. Barakos, T. Fitzgibbon, A.N. Kusyumov, et al., CFD simulation of helicopter rotor flow based on unsteady actuator disk model, CJA 33 (9) (2020) 2313–2328.
[10] H. Heyson, S. Katzoff, Induced Velocities Near a Lifting Rotor with Nonuniform Disk Loading, 1957, pp. 1–94. NACA TR 1319.
[11] V.I. Shaidakov, in: Proceedings of Moscow Aviation Institute, 68, 1978, p. 381. (in Russian).
[12] R. Steijl, G. Barakos, K. Badcock, A framework for CFD analysis of helicopter rotors in hover and forward flight, Int. J. Numer. Methods Fluids 51 (8) (2006) 819–847.
[13] Main rotor theory, General edition of A.K. Martynov, Mashinostrojenie, Moscow, 1973, pp. 1–362 (in Russian).